Article ID: 1003－6326(2004)04－0785－05

Energy-storage welding connection characteristics of rapidly solidified Cu-Co alloy foils①

XU Jin-feng(徐锦锋)[1,2], ZHAI Qiu-ya(翟秋亚)[1], JIANG Yong(蒋 永)[1]
(1. School of Materials Science and Engineering, Xi′an University of Technology, Xi′an 710048, China;
2. Laboratory of Materials Science in Space, Northwestern Polytechnical University, Xi′an 710072, China)

Abstract: The connection characteristics of rapidly solidified Cu-40% Co alloy foils were studied using a self-developed micro-type energy-storage welding machine. The results show that the microstructure of the alloy foils is characterized by uniform and fine equiaxed grains, whose maximum grain size is 1.8 μm. Under the optimum energy, the regular flat nugget is formed, low voltage and high capacitance are favorable for obtaining the perfect connection joints, whereas high voltage and low capacitance are likely to result in the surface burn of the alloy foils. With the increase of welding energy, the spot welding joint will be transformed from regular flat nugget to nugget-free one, and the microstructure tends to coarsen. The welding parameters recommended are: welding voltage 80－100 V, electric capacitance 1 800－2 500 μF, and welding force 4－8 N.

Key words: rapidly solidified alloy foils; energy-storage welding; nugget; joint microstructure
CLC number: TG 457.13 **Document code:** A

1 INTRODUCTION

Cu-Co alloy is characterized by its high mechanical properties and giant magnetoresistance (GMR) effect, and it plays an important role in the micro-electronic, automobile and aerospace industries[1,2]. Rapid solidification (RS) can make the microstructure refined remarkably, whereby obtaining the microcrystal, nanocrystal, even amorphous and metastable phase structures[3-13] with excellent properties. Therefore, RS provides a new way for further development of the potential properties of Cu-Co alloy.

The development of new materials brings about the connection problem of micro-materials. The connection methods such as hand arc welding, buried arc welding, argon arc welding, electron beam welding and diffusion welding are widely applied in engineering, but it is difficult to apply these methods to connect the low dimensional materials because of their high heat energy input, long duration of heat action and microstructure coarsening in heat-affected zone and so on. Due to its very short welding period (about 400 μs)[14,15], energy-storage welding can produce a cooling rate of 10^6 K/s with hard specifications[15], which can satisfy the microstructure coherence of the weld metal and the rapidly solidified base materials efficiently. On the other hand, since the nuggets usually crystallize under welding force, it is easy to obtain the connection joint with dense microstructures. Consequently, energy-storage resistance spot welding[15,16] is more suitable for the connection of Cu-based alloys. Up to now, the connection thickness of work-pieces to be welded by the DC shock wave resistance welder in the literature is in the range of 0.4－3.0 mm, however, few reports are given on welding work materials with the thickness less than 0.4 mm.

In the present work, the connection of the alloy foils has been conducted using a self-developed micro-type energy-storage welding machine, on the basis of manufacturing of the Cu-40% Co (mass fraction, %) alloy foils by a single roller. The ideal connection joints have been obtained, and the joint microstructure morphology and the effect of technology parameters are analyzed theoretically.

2 EXPERIMENTAL

2.1 Preparation of rapidly solidified alloy foils

The Cu-40% Co master alloy was prepared from pure Cu (99.99%) and pure Co (99.99%) by induction melting under argon atmosphere, and each sample had a mass of about 0.8－1.6 g. When an experiment began, the sample was placed in a 16 mm × 150 mm quartz test tube with d1.2 mm small holes at its bottom, and then the quartz test tube was set at the top of part of roller wheels with vacuum cover, and then vacuumed to 2.0×10^{-2} Pa, and then inversely filled with high pure Ar gas to 1.0×10^5 Pa.

① **Received date:** 2004－05－25; **Accepted date:** 2004－06－28
Correspondence: XU Jin-feng, PhD; Tel: +86-29-82312069; E-mail: xujzhai@xaut.edu.cn

This process was repeated for 3 – 5 times. The alloy was heated by high frequency heating equipment and overheated by 100K. After the temperature was maintained for 5 – 10 min, Ar gas with high pressure was blowed into the quartz tube. Meanwhile, the liquid metal was immediately sprayed onto the surface of Cu roller rotating with a high speed and formed the alloy foils with a thickness of 20 – 40 μm. In the experimental process, the linear velocity v_r of rolling wheel surface was 52 m/s.

2.2 Connection of alloy foils

After washed in the acetone, the spits on the foil surface to be welded should be scraped off so that the lapping joints could be assembled as shown in Fig. 1. The spot welding connection can be carried out on a self-developed micro-type energy-storage welding machine. In order to analyze the influence of the primary grain sizes of foils on the connecting behaviors, the surface close to the roller side (fine crystal zone) overlapped with free surface. The welding parameters included welding energy W, welding voltage U, capacitance C and welding force F. The relation among these parameters was: $W = CU^2/2$. In order to optimize the welding parameters, the single-factor experimental method was chosen. The parameters were: W = 2.0 – 15.0 J; U = 60 – 220 V; C = 150 – 2 800 μF, The welding force could be controlled in the range of 4 – 20 N. The V-422 type oscilloscope was used to monitor and control the discharge characteristics of the capacitor.

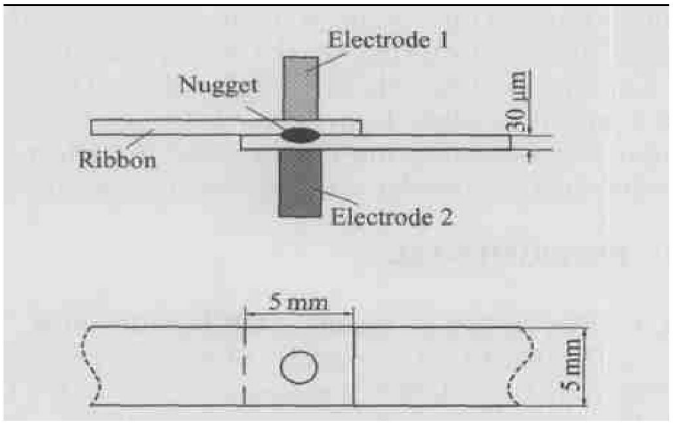

Fig. 1 Schemes of experiment method and specimens

2.3 Microstructure observation of joint

The samples of the joints were mounted in resin, polished, and etched with the solution of 5 g $FeCl_3$+ 100 mL HCl+ 100 mL H_2O. The microstructures of the joint were analyzed by XJG-05 optical microscope (OPM) and an ARMRAY-1000B scanning electron microscope(SEM). D/MAX-1200 type X-ray diffraction device (XRD) was used to analyze the phase structures of the alloy foils.

3 RESULTS AND DISCUSSION

3.1 Microstructures of alloy foils

Cu-Co alloy is a typical alloy system with peritectic transformation. The selection of the alloy composition in binary phase diagram[17] is shown in Fig. 2. In the case of the equilibrium solidification, for the Cu-40% Co alloy, the α(Co) dendrites are first crystallized from cooled melt. When the temperature reaches 1 385 K, the peritectic reaction between the interdendritic liquid and the primary α(Co) dendrites takes place, i.e. $L + \alpha(Co) \rightarrow (Cu)$. This process dominates by the atom mutual diffusion at the solid/liquid interface. The content of Co in the peritectic phase is about 7.46%. Accordingly, after the peritectic transformation, 41.2% α(Co) phase and 58.8% Cu phase will be formed. When the temperature of the alloys drops below the peritectic transformation temperature, the decrease in solubility may occur in both α(Co) phase and (Cu) phase; and when the temperature further drops to 695 K, the allotropic transformation will take place in α(Co) phase, i.e. α(Co) $\xrightarrow{695K}$ ε(Co). In addition, Cu-Co alloy is characterized by the magnetic transformation at 1 323 K.

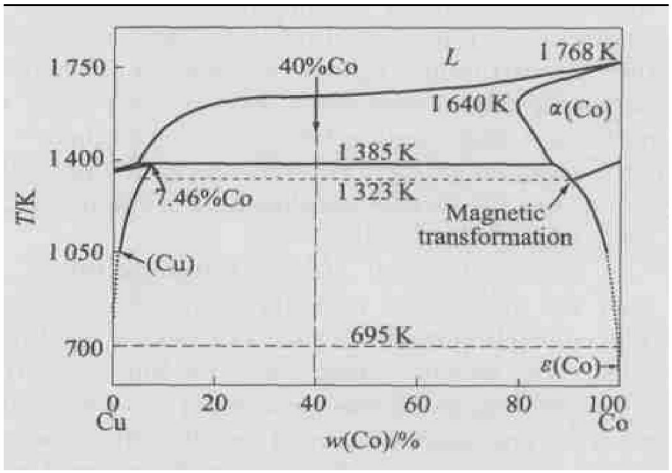

Fig. 2 Selection of alloy composition in binary phase diagram

However, under the rapid solidification condition, the microstructure and phase selection of the alloy can show the apparent deviation from that under equilibrium solidification condition, and hence the special microstructures or phase structures such as the micro-crystals, nano-crystals and even metal glass will be formed, which can cause the remarkable changes in the connection characteristic of the alloys.

Fig. 3 shows the XRD spectrum of rapidly solidified foils. It shows that even in the case of the rapid solidification, two phases of α(Co) and (Cu) are

formed. Through the contrast and analysis of α(Co) and (Cu) diffraction peaks with their standard specimens, it is found that a deviation occurs to the two kinds of diffraction peaks to some extent. It indicates that a large number of solute atoms are supersaturated in the solid solution of two phases.

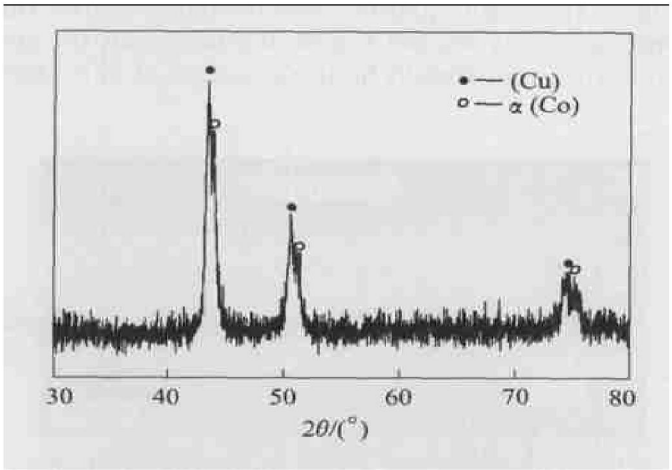

Fig. 3 XRD spectrum of alloy foils

The rapid solidification microstructure of the alloy is shown in Fig. 4. It can be classified into two zones along the thickness direction: the fine crystal zone is close to the roller surface and the free surface equiaxed zone. The thickness of the fine crystal zone is about 21 μm. In this zone, the alloy melt subjects to the chilling of the roller surface at most. The microstructure is characterized by the uniform and fine equiaxed grains with the size of 0.1 - 1.0 μm. As a result, the nearer to the roller surface, the finer the grains are.

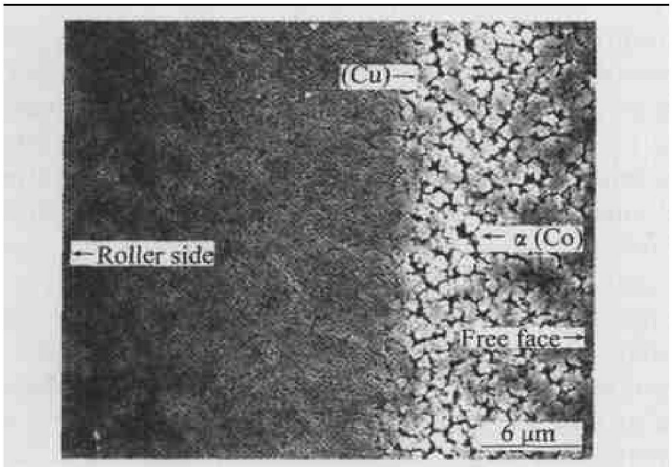

Fig. 4 Microstructure of rapidly solidified foils

The thickness of free surface equiaxed zone is about 13 μm. Due to heat resistance of the fine crystal zone and the effect of latent heat released from the solidification process, the cooling rate is dropped and the nucleation rate is reduced. Thus the grain size becomes larger, and the average size is about 1.8 μm.

3.2 Connection characteristics

3.2.1 Morphology of the joints

Fig. 5 shows the typical morphology of the spot welding joint. The welding parameters are: U = 80 V, C = 2 160 μF and W = 5.9 J. Fig. 5(a) shows the whole morphology of the joint. A regular and flat nugget is formed in the joint. There exists a bright-grey bonding line (zone) between the nugget and the base alloys. It is just the bonding line that configurates the outline of the nugget clearly. The microstructure of the base alloys adjacent to the bonding zone is still tiny equiaxed grains. The microstructure in joint is fine and dense without any defects. Fig. 5 (b) shows the magnified microstructure of the bonding zone. It can be seen that the microstructure of the nugget is quite fine, and the transition of the microstructure from nugget to base alloys is much better. In the bonding zone (about 2 - 3 grains width), the width of grain boundary becomes apparently increasing. However, the microstructure of matrix has no apparent trend to coarsening and appears to be the fine equiaxed grains.

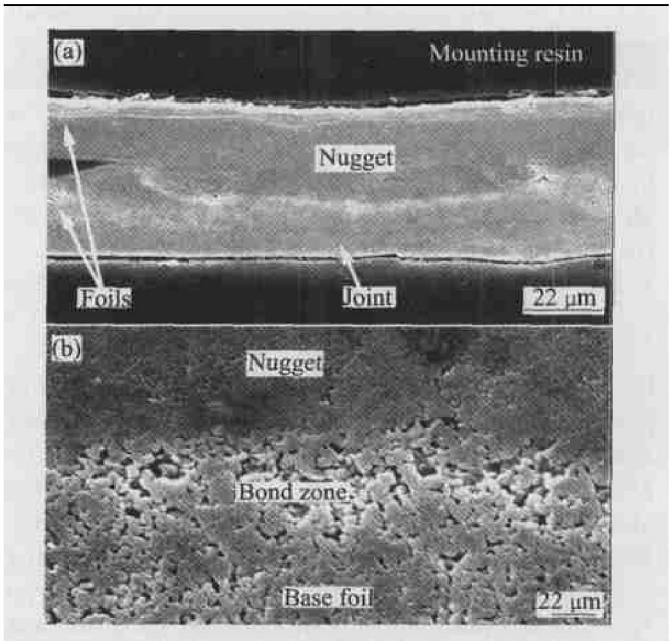

Fig. 5 Morphology and microstructure of nugget
(a) —Morphology; (b) —Microstructure

The formation of the joint microstructure is closely related to the welding conditions. In using energy-storage welding with hard specifications (large electric current, short time), the electric current produced by the instant electric discharging of the capacitance can form the electric discharge circuits, which flows through the alloy foils under welding force.

Meanwhile, the contact resistance heat produced among the foils will locally melt the base alloys to form the nugget. Largely owing to the good heat (electrical) conductivity of the alloys, the resistance heat is frequently concentrated on the contact interface of the foil surfaces. Therefore, the flat nugget is formed. Generally, the crystallization of the nugget primarily begins from the nugget/matrix boundary (semi-melting zone) with low temperature and good heat extraction condition. In this zone, the liquid phase is able to completely wet the surface of semi-melted grains with different crystallographic orientations, i. e. the wetting factors $f(\theta) \longrightarrow 0 (f(\theta) = (2+\cos\theta)(1-\cos\theta)^2/4)$, and the crystallization process possesses the minimum nucleation energy. Therefore, the undercooled liquid can attach to the crystal surface for the epitaxial growth and form the initial α(Co) grains with larger grain size and intergranular spacing, as shown in Fig. 5(b).

Owing to the micro-size of the nugget and large cooling rate, the nuggets can achieve large undercooling after the power failure so that the nucleation rate is very high. The instant nucleation and the rapid crystal growth result in the formation of rapid solidification microstructure featured with fine equiaxed crystals. At the same time, the temperature gradient of the internal nugget is so small that the nucleation and growth rate in undercooled nugget on the whole cross section tend to be identical. Thus the microstructures formed finally are homogenous. In addition, undercooled nugget is solidified under welding force, which results in the increasing of nucleation rate obviously. It is favorable for obtaining uniform and dense microstructure of the nugget.

3.2.2 Effects of welding energy on connection behavior

It is found that welding energy has a remarkable effect upon the formation of the alloy foil joints. When $W < 5.9$ J, the resistance heat is not enough to reach the local melt temperature of the alloys at contacted interface of foils. It can not realize the spot welding connection of the alloy foils. With the increase of welding energy, the melting degrees of the foils at contacted surface increase so that the morphology of joints begins to transform from the rather regular flat nugget to the uniform nugget-free one. When $W \geqslant 10.0$ J, the surface burning of the foils and electrode sticking to foils occur.

Fig. 6 shows the microstructures of nugget-free joint. Fig. 6(a) shows the overall morphology of the joint. It can be seen that the combination of the upper and lower parts of the alloy foils is good. The joint is the typical nugget-free spot welding joint. Fig. 6(b) shows the center microstructure of the joint. It reveals that the microstructure is more coarsening than that of regular nugget shown in Fig. 5(b). The size of α(Co) grains is about 5 μm, even larger than the size of equiaxed grains in the alloy foils near free surface. In the cross section of the joint, the microstructure is homogenous. This indicates that with the increase of the welding energy, the overheating of the foils increases and the cooling rate of the joint decreases, correspondingly, the coarse microstructure forms. Thus, for obtaining the high quality spot welding joint, the welding energy should not be too large and the appropriate value should be in the range of 5.9 – 8.0 J.

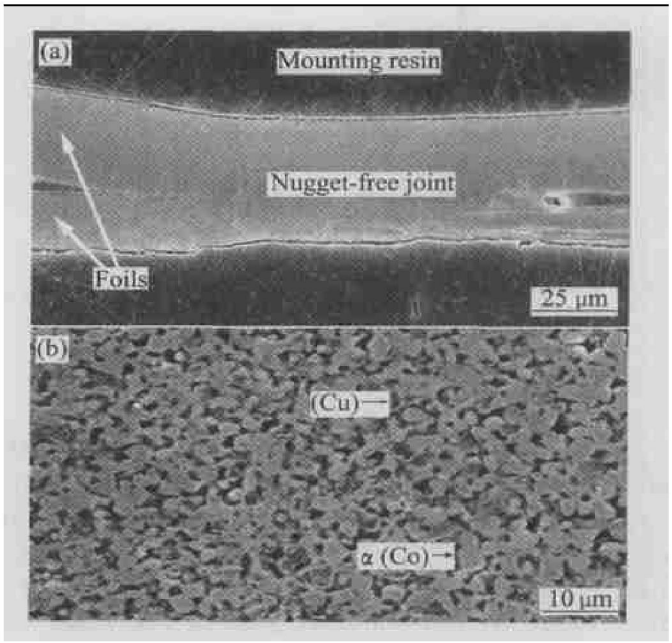

Fig. 6 Morphology and microstructure of joint under high welding energy
(a) —Morphology; (b) —Microstructure

After all, there exists great difference between the micro-type energy-storage welding and traditional electric resistance welding in the connection of foils. Since the welding period is much shorter than the resistance welding[7], the process of joint formation for energy-storage welding still belongs in the category of rapid solidification though greater welding energy is applied. Therefore, the phase separation of Cu-Co alloy does not occur during welding, which usually takes place under equilibrium condition. The primary α(Co) phase is still characterized by homogenous fine equiaxed grains, and some peritectic (Cu) phases distribute at the grain boundary of α(Co). It is no doubt that these microstructures play an important role in maintaining the GMR effects of Cu-Co alloys.

3.3 Optimization of connection parameters

The relationships among the welding voltage, capacitance, and joint qualities are listed in Table 1. It indicates that the combinations of low voltage and high capacitance are favorable for obtaining the ideal connection joints, while high voltage and low capaci-

tance are liable to cause the surface burn of alloy foils, which can seriously affect the welding qualities. Accordingly, in the case of fixing the welding energy and welding force, using the welding specifications with low voltage and high capacitance is easy to obtain high quality spot welding joints. The recommended welding parameters are: welding energy 5.9 – 8.0 J, welding voltage 80 – 100 V, electric capacitance 1 800 – 2 500 μF, and welding force 4 – 8 N.

Table 1 Effects of welding parameters on quality of joint

W/J	Low voltage and high capacitance			High voltage and low capacitance		
	U/V	C/μF	Joint quality	U/V	C/μF	Joint quality
5.9	80	1 844	Good	247	194	Surface burn
6.5	90	1 605	Good	198	330	Surface burn
6.9	100	1 380	Excellent	204	332	Severe burn

4 CONCLUSIONS

1) The micro-type energy-storage welding is able to realize the spot welding connection of Cu-Co alloy foils, and the perfect connection joints are obtained.

2) In the case of fixing welding energy, using low voltage and high capacitance is favorable for obtaining high quality spot welding joints. With the increase of the welding energy, the morphology of the joints begins to transform from the regular flat nugget to the nugget-free one, and the microstructure of joint tends to coarsen.

3) The recommended welding parameters are: welding voltage 80 – 100 V, electric capacitance 1 800 – 2 500 μF, and welding force 4 – 8 N.

Acknowledgements

The authors would like to express the heartfelt thanks to Professor WEI Bing-bo to offer the benefit help. The authors also thank Professor WANG Nan, Dr. XIE Wen-jun, Dr. LÜ Yun-jun and Dr. LIU Xiang-rong for their useful discussion.

REFERENCES

[1] SUN Zhan-bo, SONG Xiao-ping, HU Zhu-dong, et al. Effects of earth additions on GMR of melt-spun Cu-Co-Ni ribbons[J]. Journal of Magnetism and Magnetic Materials, 2001, 234(2): 279 – 283.

[2] Song X, Mahon S W, Cochrane R F, et al. Microstructural evolution and giant magnetoresistance in melt-spun $Cu_{70}Co_{30}$ ribbon[J]. Journal of Alloys and Compounds, 1996, 245(1 – 2): 75 – 79.

[3] LI D, Robinson M B, Rathz T J, et al. Direct determination of the metastable liquid miscibility gap in undercooled Cu-Co alloys[J]. Materials Letters, 1998, 36(1 – 4): 152 – 156.

[4] SUN Zhan-bo, SONG Xiao-ping, HU Zhu-dong, et al. Liquid separation behavior of Cu-Co alloys under deep supercooling[J]. The Chinese Journal of Nonferrous Metals, 2001, 11(1): 68 – 73. (in Chinese)

[5] SUN Zhan-bo, SONG Xiao-ping, HU Zhu-dong, et al. Secondary liquid separation and solidification of Cu-Co alloys under deep supercooling[J]. The Chinese Journal of Nonferrous Metals, 2001, 11(2): 172 – 175. (in Chinese)

[6] CAO Chong-de, WANG Nan, WEI Bing-bo. Containerless rapid solidification of undercooled Cu-Co peritectic alloys[J]. Science in China(series A), 2000, 43(12): 1318 – 1326.

[7] LIU Yuan, LI Yan-xiang, GUO Jing-jie, et al. Liquid phase separating mechanism and preparation techniques of immiscible alloys[J]. Trans Nonferrous Met Soc China, 2002, 12(3): 357 – 365.

[8] ZHAO Jiu-zhou. Model for calculation of microstructural development in rapidly directionally solidified immiscible alloys[J]. Trans Nonferrous Met Soc China, 2002, 12(3): 366 – 369.

[9] Yamauchi I, Ohmori M, Ohnaka I. Metastable phase formation by chemical leaching of Al-Co-Cu ternary alloys [J]. Journal of Alloys and Compounds, 2000, 299 (1 – 2): 269 – 275.

[10] Bosco E, Rizzi P, Baricco M. Rapid solidification of immiscible alloys[J]. Journal of Magnetism and Magnetic Materials, 2003, 262(1): 64 – 68.

[11] Busch R, Gärtner F, Borchers C, et al. High resolution microstructure analysis of the decomposition of $Cu_{90}Co_{10}$ alloys[J]. Acta Mater, 1996, 44(6): 2567 – 2579.

[12] Robinson M B, Li D, Rathz T J, et al. Undercooling, liquid separation and solidification of Cu-Co alloys[J]. Journal of Materials Science, 1999, 34(15): 3747 – 3753.

[13] Munitz A, Abbaschian R. Liquid separation in Cu-Co and Cu-Co-Fe alloys solidified at high cooling rates[J]. Journal of Materials Science, 1998, 33(14): 3639 – 3649.

[14] ZHANG Sheng-yu. Welding of titanium-based composites[J]. Welding Technology, 2000, 29(5): 49 – 50.

[15] Ellis M B D. Joining of aluminium based metal matrix composites[J]. International Materials Reviews, 1996, 41(2): 41 – 58.

[16] ZHANG Y, Taylor D. Optimization of spot-welded structures[J]. Finite Elements in Analysis and Design, 2001, 37(12): 1013 – 1022.

[17] Massalski T B, Murray J L, Bennett L H, et al. Binary Alloy Phase Diagrams[M]. Ohio: ASM International, 1990. 1181 – 1183.

(Edited by LI Xiang-qun)